International Journal of Engineering Trends and Technology
ISSN: 2231-5381/ https://doi.org/10.14445/22315381/IJETT-V74I5P136

Volume 74 Issue 5, 577-597, May 2026

Original Article

AI-Based Correlation Analysis of Torque and Vibration for Misalignment Fault Detection in Rotating Machinery

Amruta Vaibhav Adwant[1, 2], Manpreet Singh[2], Suhas Deshmukh[3]

[1]*Mechanical Engineering, Dr. D. Patil International University, Pune, India.*
[2] *Mechanical Engineering, Lovely Professional University, Punjab, India.*
[3]*Government College of Engineering, Karad, Maharashtra, India.*

[1]*Corresponding Author : amruta.adwant@gmail.com*

Received: 25 January 2026 Revised: 04 March 2026 Accepted: 11 March 2026 Published: 30 May 2026

Abstract - *Shaft misalignment is a prevalent issue in rotating machinery. The majority of individuals initially overlook this issue due to the relatively low vibration amplitudes, and conventional vibration-based diagnostics are not very adept at detecting them. This study investigates the relationship between torque and vibration data to enable precise diagnosis of misalignment issues in real operational conditions. A test rig was built to gather real-time data on torque and vibration in both aligned (0°) and misaligned (0.5°–2°) states. It had a shaft made of A36 steel, torque estimates based on encoders, and piezoelectric accelerometers. Principal Component Analysis was performed to get rid of and reduce features in the time, frequency, and cross-domains. After that, Support Vector Machine, Random Forest, and Convolutional Neural Network models were used to group the errors. The results show that misalignment causes a lot of harmonic amplification and less torque-vibration coherence. This is shown by the fact that correlation values drop from about 0.95 in aligned conditions to 0.65 in misaligned conditions. The combination of deep learning and multisensory fusion was proven to be better by the classification accuracies of 91.3%, 93.2%, and 95.7% reached using SVM, RF, and CNN models, respectively. The primary innovative feature of this study is how it combines torque and vibration characteristics from an encoder with knowledge of physics and geometry. Because of its integration, low-angle misalignment (0.5°) can be precisely identified, even though vibration-only approaches usually miss it. A scalable and easy way to forecast when rotating gear needs maintenance is provided by this approach to incorporating torque and vibration. It also improves the longevity of models across different shaft shapes and facilitates early issue identification.*

Keywords - *Torque-Vibration Correlation, Rotating Machinery, Support Vector Machines, Random Forest, Convolutional Neural Networks, Vibration Signatures, Time-Frequency Spectrogram, Fast Fourier Transform.*

1. Introduction

Rotating equipment is very important to the manufacturing, energy production, transportation, and aviation industries. The shafts must be perfectly aligned for these systems to work properly and be reliable. Shaft misalignment, whether angular or parallel, is a typical problem in devices that spin. Higher bending strains, cyclic loading, excessive vibration, bearing wear, and nonlinear torque transfer can result from even small angle changes. Improperly oriented equipment can have unexpected issues, consume more energy, and break down sooner. For a long time, vibration analysis has been the greatest way to find things that are out of sync. Time-domain statistical characteristics, frequency-domain analysis using the Fast Fourier Transform (FFT), and time-frequency approaches like the Wavelet Transform have all found harmonics and amplitude modulation patterns that are linked to misalignment. Vibration-based diagnostics are good at finding big problems, but they might not be as good at finding little misalignments. The vibration amplitudes may be so small at first that they are hard to see because of noise in the background or structural dampening. The vibration signatures might change depending on the shape, stiffness, and load distribution of the Shaft. This makes them less reliable in different mechanical circumstances. Torque, on the other hand, tells you how much weight the Shaft can support directly. Classical torsion theory explains how shaft rigidity, angular displacement, and torque are all related to each other. It helps you understand how things move in a physical way. When pieces are not lined up correctly, harmonic distortion and torque changes arise at regular intervals due to problems with nonlinear load transmission and coupling. Changes in vibration amplitude may demonstrate how an issue is getting worse, and changes in torque may show changes in the mechanical power being sent. This could mean that defects show up sooner than expected. Even though torque is significant in real life, much of the research done so far either does not look at it at all or only looks at vibration diagnostics. Now, there is an absence

of comprehensive research examining the correlation between torque and vibration as diagnostic indicators for shaft misalignment. There has been inadequate research on the quantitative evaluation of correlation deterioration in regulated low-angle misalignment scenarios. The combination of machine learning methods for classifying defects with physically based torque prediction in experimental rotating shaft systems is still in the early stages of development.

In recent years, advancements in machine learning have simplified the process of automating fault classification. Support Vector Machines (SVM), Random Forests (RF), and Convolutional Neural Networks (CNN) are among the techniques that have been effective in identifying nonlinear patterns in vibration data. However, exclusively data-driven models may not be physically comprehensible and may have issues when applied to small datasets or systems that rely on geometry. By incorporating physically pertinent signals such as torque into the learning system, it may be possible to enhance its resilience while maintaining its mechanical simplicity.

Although much research has been conducted on vibration-based misalignment detection methods, the majority of it exclusively examines vibration amplitude or frequency-domain features and does not incorporate transmitted torque data. This reduces the sensitivity to low-angle misalignment and limits physical interpretability in constant-speed scenarios. Additionally, numerous investigations have failed to statistically investigate the absence of torque–vibration correlation as a diagnostic criterion. It is important to establish a physics-based fusion framework that uses vibration signals to estimate torque and tests its performance through data-driven modeling.

This study's primary contributions are:

- Experimental evaluation of torque-vibration correlation degradation under controlled misalignment (0.95 → 0.65).
- Combining vibration feature extraction and encoder-based torque estimates in a geometry-aware framework.
- Early-stage misalignment detection at 0.5 degrees is demonstrated.
- Using machine learning models with specified repeatability parameters for quantitative validation.

This paper presents a physics-informed, dual-sensor diagnostic system that combines encoder-derived torque estimation with vibration signal analysis for detecting shaft misalignment. Torque is calculated using traditional torsion equations derived from observed angular displacement, whereas vibration signals are analyzed to obtain statistical and frequency-domain characteristics. The relationship between torque and vibration is statistically assessed under both aligned and misaligned situations (0.5° and 2°) at a constant rotating speed of 600 RPM.

This paper presents a physics-informed, geometry-aware framework for torque-vibration fusion aimed at the early detection of misalignment under regulated operating conditions. This study experimentally quantifies correlation degradation and validates the effectiveness of AI-based classification and regression, thereby bridging the divide between mechanical modeling and data-driven diagnostics and providing a reproducible and interpretable solution for predictive maintenance applications.

1.1. Literature Survey and Research Gap

Vibration-based diagnostics have long been used to monitor the condition of rotating machinery. Time-domain statistical features such as Root Mean Square (RMS), kurtosis, skewness, and crest factor, together with frequency-domain techniques based on the Fast Fourier Transform (FFT), are widely applied for shaft misalignment and imbalance detection [1-3]. Randall [1] established the foundation for vibration-based condition monitoring, while Antoni [2] demonstrated the effectiveness of spectral kurtosis in detecting non-stationary mechanical faults. Lei et al. [3] presented a systematic review of intelligent machinery health prognostics methods for industrial rotating systems.

Recent studies have improved diagnostic sensitivity through advanced signal processing and dimensionality-reduction methods. Deng et al. [4] integrated Variational Mode Decomposition (VMD) with PCA-SVM for incipient bearing fault identification. Zhang et al. [5] proposed entropy-based machine-learning methods for rotating machinery fault diagnosis, whereas Jiang et al. [6] combined PCA and Convolutional Neural Networks (CNN) for planetary gearbox diagnostics.

Deep learning approaches are increasingly being adopted for automated fault classification. Ong et al. [7] demonstrated the effectiveness of deep CNN models for vibration-based health monitoring of rotating machinery, while Fu et al. [8] developed adaptive CNN architectures for bearing fault diagnosis under noisy conditions. Zhang et al. [9] reviewed deep-learning-based rotating machinery fault diagnosis and highlighted limitations associated with interpretability and large data requirements.

Multi-sensor fusion techniques have also gained attention in intelligent diagnostics. Elsamanty et al. [10] improved fault detection reliability using fused vibration and electrical signals with PCA, whereas Rodrigues et al. [11] applied machine-learning classification using vibration orbit spectrum images. However, most existing fusion frameworks remain largely data-driven and lack physical interpretability. Torque-based diagnostics have received comparatively less attention. Pérez et al. [12] investigated torsional vibration measurement

techniques in rotating shafts and showed that torque variations reflect changes in shaft stiffness and dynamic loading. Adwant et al. [13] developed a portable dynamic torque measurement system capable of capturing real-time torque fluctuations in rotating systems. Nevertheless, torque-derived features are still rarely integrated with AI-based misalignment detection frameworks.

Machine-learning algorithms such as Support Vector Machines (SVM) [14], Random Forests (RF) [15], and intelligent fault diagnosis methods under noisy or imbalanced conditions [16] have demonstrated strong classification capability in rotating machinery applications. Feature-engineering approaches for AI-supported fault diagnosis were further discussed by Zhang et al. [17]. Acoustic and vibration-based intelligent monitoring approaches have also been reported by Glowacz [18]. More recently, multi-sensor fusion frameworks [19], intelligent diagnosis under imperfect data conditions [20], and transfer-learning approaches for varying operating conditions [21], [22] have significantly improved model robustness and cross-domain generalization.

Despite these developments, several important limitations remain. Most existing studies rely primarily on vibration-only diagnostics and do not integrate encoder-derived torque information into AI-driven fault classification systems. Quantitative analysis of torque-vibration correlation degradation under low-angle misalignment conditions is still limited. Furthermore, few studies provide geometry-aware and physics-informed diagnostic frameworks capable of detecting early-stage misalignment with high interpretability.

1.1.1. Identified Research Gap

The literature reveals the following limitations:

- Heavy dependence on vibration-only diagnostic systems.
- Limited incorporation of encoder-derived torque in AI-driven misalignment detection.
- Lack of quantitative correlation analysis between torque and vibration signals.
- Inadequate validation of early-stage low-angle misalignment (≤0.5°).
- Limited development of geometry-aware and physics-informed diagnostic frameworks.

This study addresses these gaps by experimentally quantifying torque-vibration correlation degradation and validating a dual-sensor, physics-informed framework using SVM, Random Forest, and CNN models.

2. Methodology and Models

A typical experimental test setup was built with A-36 steel shafts, as shown in Figure 1. A unique experimental test rig was made with A-36 steel shafts that were 10 mm to 15 mm wide and 500 mm to 750 mm long. During this study, a 5 HP variable-speed motor that ran steadily at 600 RPM drove the Shaft. The gadget used both stiff and flexible couplings to show how shafts could be aligned or misaligned. To keep an eye on vibration, the ADXL1002 piezoelectric accelerometers were attached to bearing housings. To measure torque, an in-line torque sensor called the TQX-05, which was very sensitive at 0.01 Nm, was employed. A National Instruments DAQ system connected to LabVIEW collected all of the sensor data in real time. An E6B2-CWZ6C optical encoder provided precise rotational displacement data. Table 1 shows the exact features of the sensors utilized in the experiment.

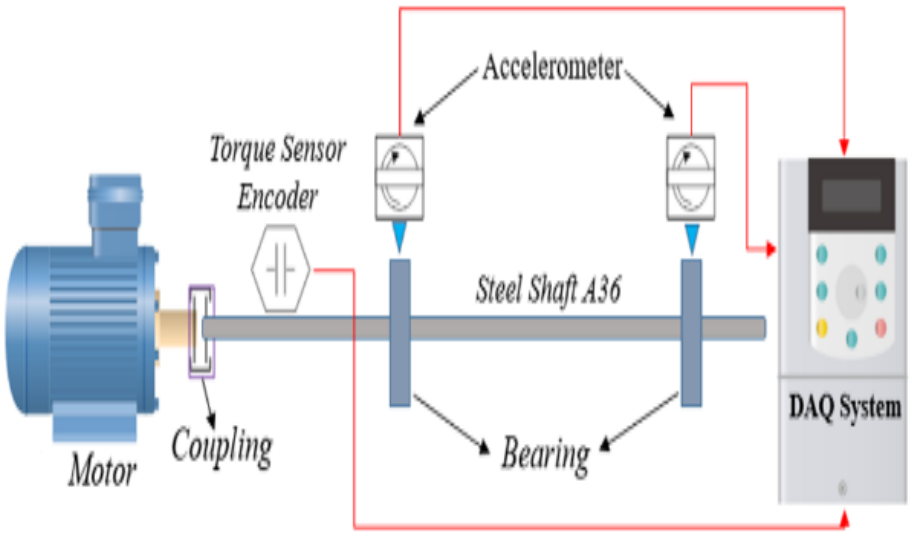

Fig. 1 Experimental setup for torque and vibration monitoring

Table 1. Detailed specifications of sensors used in experimental setup

Sensor Type	Model	Measurement Range	Sensitivity	Accuracy	Mounting Location	Application
Accelerometer	ADXL1002	±50 g	100 mV/g	±2%	Bearing Housing	Vibration Signal Acquisition
Torque Sensor	TQX-05	±100 Nm	0.01 Nm	±0.1%	In line with Shaft	Dynamic Torque Measurement
Optical Encoder	E6B2-CWZ6C	1000 PPR	–	±0.5°	Shaft End	Rotational Displacement (Angle)

2.1. Shaft Alignment and Misalignment Simulation

The experimental rig was tested in two main alignment conditions: aligned and misaligned. This was done to find out how well the equipment worked and how well it performed. The rods were parallel to each other and at an angle. With the high-precision laser shaft alignment method, you can acquire the right alignment and a solid baseline. The connecting flange was purposely tilted to make the difference that was needed. People thought that 2.0° and 0.5° misalignments were relevant. This angle is useful for validating the accuracy and sensitivity of fault detection systems because it is similar to angles used in industry.

2.1.1. Misalignment Introduction and Measurement

In a controlled environment, a shaft that is misaligned can be generated using A Precise Mechanical Simulator (SIM). This procedure makes it possible to completely blend angular and parallel misalignments in the component of the test rig that connects. The tools made this happen. To make angular misalignments of 0.5 to 2.0 degrees, calibrated spinning fixtures were employed on purpose.

To locate and verify the misalignment, a precise angle measuring device with an accuracy of ±0.1° was used. After following the provided testing steps, this method was successfully repeated numerous times. Before collecting data, each setup was locked and checked to make sure that noise and other sources of interference would not affect the torque and vibration signals. This setup makes sure that sensor data will not be affected by shaft misalignment. When connected to 240V and 50Hz, a 5 HP induction motor can handle 0.5 Nm of power. Up to 1500 times per minute, the engine can turn. To make it more like working at low speeds in an industrial setting, it was run continuously at 600 RPM for this job. This cuts down on inertial disturbances. The closed-loop control system in this machine kept changes in speed and force stable when pulses were sent to it. Slip-fit SIM plugs that have been measured, and angular tools that are accurate to within 0.05°, were used to fix the Shaft that was not lined up correctly.

Table 2 displays a complete test matrix that will be used to thoroughly verify how well the system functions in many areas, like the diameter of the Shaft, the speed of rotation, and the angles of set misalignment.

All investigations were conducted at a fixed rotating speed of 600 RPM under steady-state circumstances. The motor was controlled by a closed-loop system that used encoder feedback to keep speed changes to a minimum and get rid of torque ripple. During the studies, a steady mechanical load condition was maintained. This study does not include scenarios with variable speed and load. This controlled design made sure that the changes in torque and vibration signals that were found were only caused by the Shaft being out of alignment, not by changes in how the machine was working. There were five distinct angles of misalignment (0°, 0.5°, 1°, 1.5°, and 2°) and five different amounts of torque (20–100 Nm) employed in the tests. The speed of rotation stayed at 600 RPM. This design makes it easy to see how well a model performs when the load and shape change, while maintaining the same speed to show how misalignment affects the model.

Table 2. A full list of the experimental test matrix.

Test Case	Alignment Type	Speed (RPM)	Shaft Diameter (mm)	Misalignment (°)	Torque Level (Nm)
A1	Aligned	600	10	0	20–100
M1	Misaligned	600	10	0.5	20–100
M2	Misaligned	600	10	1.0	20–100
M3	Misaligned	600	10	1.5	20–100
M4	Misaligned	600	10	2.0	20–100

2.2. Torque and Vibration Measurement Technique

The torque value was accurately determined by the torsion formula when applied to the encoder-based angular displacement. The following math will help you find out the torque:

$$\frac{T}{J} = \frac{G\,\theta}{L} \tag{1}$$

Torque is measured in Nm, polar moment of inertia is measured in m⁴, shear modulus of A36 steel is about 79.3 GPa,

angular displacement is measured in radians using an encoder, and shaft length is measured in meters. The accelerometer data was converted into speed and distance via numerical integration.

To find important failure signs in both the temporal and frequency domains, modern signal processing methods like the Fast Fourier Transform (FFT) and the Wavelet Packet Transform (WPT) were used.

Signal Acquisition and Filtering

At 5 kHz, a 16-bit National Instruments data gathering device collected all of the torque and vibration signals. The sample frequency chosen meets the Nyquist requirement and offers decent resolution for harmonic parts up to 2.5 kHz. Before the data was collected, analog anti-aliasing low-pass filtering was done at 2 kHz. A digital Butterworth low-pass filter (4^{th} order, with a cutoff frequency of 200 Hz) was also utilized in the preprocessing phase to get rid of high-frequency noise that had nothing to do with shaft dynamics.

Table 3. Key formulas and techniques for torque and vibration analysis

Measurement Type	Parameter	Formula / Technique	Description
Torque	Torque (T)	$T = \frac{G\,\theta\,J}{L}$	Calculating torque from angular displacement
Vibration	Displacement (x)	$x(t) = \iint a\,(t)\,dt$	Double integration of acceleration (a) to obtain displacement
Frequency-domain	FFT	$X(f) = \int_{-\infty}^{+\infty} x(t)e^{-j2\pi ft}dt$	Extracting frequency components from vibration signals
Time-frequency	WPT	Wavelet disintegration	Recognizing momentary and contained features

2.2.1. Encoder-Derived Torque Estimation and Validation

Two complementary approaches were used in this work to assess torque: (i) direct measurement using a calibrated dynamometer, and (ii) estimation using an encoder that applied the torsion formula. To measure the angle of rotation (θ) while the Shaft was moving, a rotary encoder with 5000 pulses per revolution (PPR) was mounted on it. The formula

$$\theta = \frac{Pulse\ Count}{5000} \times 2\pi \quad (2)$$

was used to turn the number of encoder pulses into an angle. This displacement was later used in the standard torsion Equation (1).

As part of this research, shafts with different sizes and lengths (500 mm, 600 mm, and 700 mm) were used. The model was proven to be accurate when the torque values from real-time encoder data nearly matched the dynamometer results (within a range of ±1-3 Nm).

The optical encoder used in this study has an angular resolution of ±0.5°. The uncertainty in torque estimation was evaluated using error propagation.

$$\Delta T = \frac{G\,J}{L}\Delta\,\theta \quad (3)$$

Based on shaft geometry and material properties, the propagated uncertainty in torque estimation was estimated to be within ±2.8%. This is consistent with the experimentally observed ±1–3 Nm deviation between encoder-derived torque and dynamometer measurements. In this study, a multimodal AI diagnostic pipeline to estimate torque based on physical principles was used. Previous research relied solely on Black-Box Models or Vibration Signals to identify geometry-sensitive early-stage problems like 1.0° misalignment. This approach uses a well-established mechanical torque model along with vibration-domain features to address this issue. The encoder-to-torque formulation enhances the transparency of intelligent decision-making and raw sensor data, hence improving diagnostic performance and clarity. This employs unique mechanics utilizing encoders for real-time fault categorization.

The agreement between encoder-derived torque and dynamometer data was statistically evaluated using Root Mean Square Error (RMSE), Mean Absolute Error (MAE), and the coefficient of determination (R^2). The encoder-based torque estimation system was proven to be strong and reliable because R^2 was always over 0.97 and RMSE was always below 3 Nm.

The raw data from the torque and vibration monitor is now available so that anyone may readily duplicate the results. There are more than 120 possible ways to build up operations with this substance. There is a different set of shaft diameters, length, weight, and offset angle for each dataset file.

These files give you the raw signals from the encoder and the accelerometer. The dataset's Python utilities do a lot of things on the signals, such as window segmentation, normalization, and low-pass filtering at 200 Hz. This enables you to apply the same methods to figure out torque and combine signals again. Even though the factorial design is done in a lab, it makes it easier to see several kinds of machine failures that could happen in real life.

2.3. Scope of Theoretical Framework and Dynamic Considerations

The relationship between transmitted torque and vibration characteristics in a rotating shaft system is examined in this work using an experimental and data-driven methodology.

Classical torsion theory, on which torque measurement is based, states that the applied torque and the Shaft's angular twist are connected in the following manner of the torsional equation Equation (1). It is simple to determine the torque immediately since the novel optical probe continuously measures the twist angle.

The testing apparatus has accelerometers that record vibration signals in an actual environment. The unprocessed vibration time-domain data is used to compute statistical measures like mean, RMS, standard deviation, kurtosis, skewness, crest factor, and peak amplitude. These metrics are then utilized as input characteristics for AI-based torque forecasting models and for correlation analysis. Inertia-stiffness-damping correlations frequently clarify the dynamics of a rotating shaft; nonetheless, this work does not aim to develop or solve a thorough analytical equation of motion using Lagrangian mechanics. The primary objective is to utilize scientific methods to elucidate the relationship between torque and vibration features, and to evaluate the efficacy of data-driven AI systems in predicting torque. The work is structured as an experimental-empirical inquiry based on classical torsion theory, rather than a thorough analytical dynamic modeling assessment.

2.4. Signal Processing and Data-Driven Validation Framework

A quantitative correlation analysis was conducted by analyzing the torque and vibration signals to extract time-domain, frequency-domain, and cross-domain components. Statistical analysis was employed alongside data-driven models to assess the prediction efficacy of vibration-derived features in evaluating transmitted torque and distinguishing alignment circumstances. The purpose of this method is to show how useful torque-vibration correlation may be for diagnosis using machine learning, not to come up with a new way to find defects.

To ensure the accuracy and reliability of torque and vibration data, accelerometers, torque sensors, and optical encoders are meticulously positioned within the experimental configuration. Signal pre-processing, which includes removing noise, filtering, and removing artifacts, makes signals better for analysis once they have been collected. Next, apply advanced signal processing methods like FFT, WPT, and statistics to get features. It would be helpful to extract common and diagnostic features from processed data in order to better understand functioning statuses and failure situations. Feature Fusion and Normalization combine and normalize the features that have been found. This combines domain features into a single dataset so that data from different sources may be compared and consistent. The dataset becomes more valuable after normalization. Machine Learning Model Training uses complex algorithms like SVM, RF, and CNN to find patterns and sort operational states. The Principal Component Analysis (PCA) on all of the retrieved features (time-domain, frequency-domain, and cross-domain) was applied to reduce the number of features and make the model more general.

2.4.1. Principal Component Analysis

Principal Component Analysis (PCA) was utilized to diminish dimensionality while maintaining the dataset's most informative characteristics, which included multiple time-domain, frequency-domain, and cross-domain features, including RMS, Shannon entropy, spectral entropy, skewness, kurtosis, and harmonic indicators. The explained variance ratio was figured out for each major component, and a scree plot (Figure 2) was created to show it. This reduction in dimensionality not only made the feature space simpler to deal with but also enabled the calculations to be completed more quickly while maintaining a good level of classification performance across all models. The top five principal components were provided as input features to both the Support Vector Machine (SVM) and Random Forest classifiers. Regarding the total variation, these components were responsible for approximately 73.1% of it. This resulted in a reduction in redundancy and assisted in preventing the model from overfitting, which was particularly helpful when working with small datasets.

The total explained variance ratio of the primary components that were identified from the torque and vibration feature set is illustrated in Figure 3. The cumulative curve illustrates that the initial five primary components account for approximately 73.1% of the total changes. The variance remains relatively constant following the fifth component. This implies that the retention of additional components does not enhance returns. To assist the SVM and Random Forest classifiers in achieving a balance between preserving information and simplifying it, the initial five components were selected as inputs. Finally, trained algorithms that can tell the difference between normal and defective circumstances, such as shaft misalignment, are used to classify and anticipate problems. A full Performance Evaluation looks at how well the model can find mistakes and make assumptions.

Figure 4 illustrates how accuracy and recall are assessed. Numerous simulations were run for aligned and misaligned shaft designs to determine how misalignment affects spinning machinery. Laser alignment showed that the shafts were completely aligned with no angular or parallel deviations. Next, controlled angular deviations were used to make the connecting flange appear out of alignment at particular offset angles. Moderate (0.5°) and severe (2.0°) operational circumstances were examined in this study.

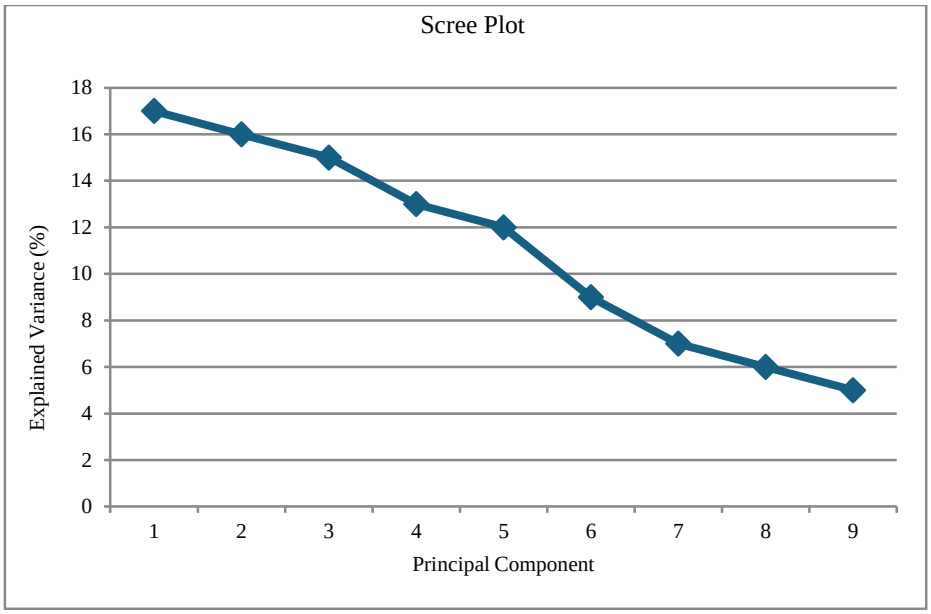

Fig. 2 Scree Plot: Explained variance by principal components

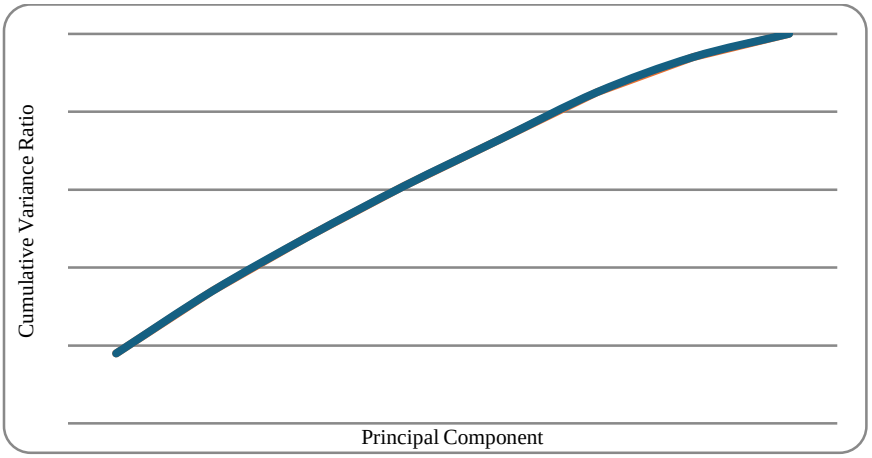

Fig. 3 Cumulative explained variance by principal components

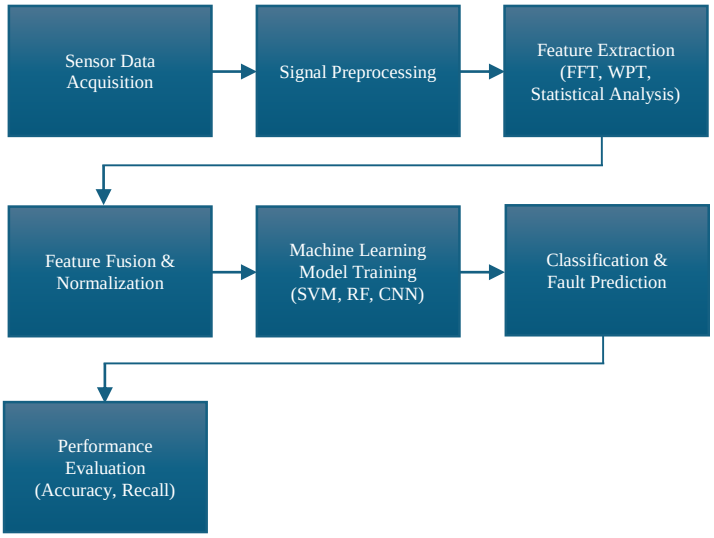

Fig. 4 Signal processing and machine learning analysis workflow

Making a setting that is an accurate representation of the real world. This study is able to ascertain the effect of misalignment on the torque and vibration measurements by analysing the outcomes of these different instances. As a result, effective predictive maintenance approaches for industrial rotating gear were created by merging precise correlation analysis with comprehensive simulation.

Table 4 shows the two most important extracted features, together with their domain and usage definitions.

Table 4. Extracted features for signal processing and fault diagnosis

Feature Domain	Extracted Features	Description/Usage
Time-domain	Root Mean Square (RMS)	Specifies total signal extent or power
	Peak-to-Peak Amplitude	Signifies extreme amplitude dissimilarities in signals
	Standard Deviation	Dealings signal dispersal or unpredictability.
Frequency-domain	Dominant Frequencies	Recognizes primary frequency components associated with accountabilities
	Harmonics	Notices multiples of fundamental incidences
	Sidebands	Specifies variation effects from faults or misalignment
Statistical	Skewness	Measures asymmetry in signal distribution
	Kurtosis	Estimates peakedness, useful for anomaly finding
Cross-domain	Torque-Vibration Coherence	Measures the connection between torque and vibration signals
	Correlation Coefficients	Measures the strength of torque-vibration associations

2.4.2. Machine Learning-Based Validation

This part makes it apparent what the model settings, hyperparameters, and training processes are for all machine learning techniques. This makes sure that the methods are explicit and can be repeated.

Data Partitioning and Validation Strategy

The dataset was divided into two parts, with 80% for training and 20% for testing. This was done to make sure that the model was evaluated fairly and to avoid overfitting. The proportion of aligned and misaligned classes was kept the same in both parts.

A validation set was established from 20% of the 80% training data to evaluate the generalizability of the model during CNN training. This made it easy to share data of:

- 64% Training
- 16% Validation
- 20% Testing

In order to prevent overfitting, the validation set was employed to monitor validation loss and implement early halting (patience = 10 epochs).

A five-fold cross-validation was implemented on the training data to optimize the hyperparameters of the Support Vector Machine and Random Forest models. The independent 20% test set was only used to evaluate the model's final performance and not during training or hyperparameter adjustment. This stopped data from leaking. To make sure that the results could be repeated, all divisions were done using a fixed random seed (42).

2.5. Support Vector Machine (SVM)

The Support Vector Machine classifier was run with the Radial Basis Function (RBF) kernel, which works very well for nonlinear classification in feature spaces with a lot of dimensions.

Grid search and 5-fold cross-validation were used to fine-tune the hyperparameters. The setup that was picked is as follows:

- Kernel: Radial Basis Function (RBF)
- Regularization parameter (C): 1.0
- Kernel coefficient (γ): 'scale.'
- Tolerance for stopping criterion: 1×10^{-3}
- Maximum number of iterations: 1000

The best hyperparameters were found by finding the highest mean cross-validation accuracy. To make the SVM model broader and faster, it used PCA-reduced features as input.

2.5.1. Random Forest (RF)

The Random Forest classifier was used as an ensemble learning method that could handle nonlinear correlations and interactions between features in torque-vibration data.

Grid search with 5-fold cross-validation was used to find the best hyperparameters. The parameters that were chosen are:

- Number of trees (n_estimators): 100
- Maximum tree depth (max_depth): 15

- Minimum samples required to split a node (min_samples_split): 2
- Minimum samples required at a leaf node (min_samples_leaf): 1
- Splitting criterion: Gini impurity
- Bootstrap sampling: Enabled
- Random state: 42

The final classification output was determined through majority voting across all decision trees.

Convolutional Neural Network (CNN)

A Convolutional Neural Network (CNN) was created to independently pull out spatial-frequency representations from time-frequency spectrogram inputs that came from torque and vibration data.

Input Configuration

- Input type: Time–frequency spectrogram
- Input dimensions: 128 × 128 × 1
- Input normalization: Min–max scaling applied independently to each sample

CNN Architecture

The CNN architecture consisted of three convolutional blocks followed by fully connected layers. The detailed layer-wise configuration is provided below:

1. Conv2D Layer
- Filters: 32
- Kernel size: (3 × 3)
- Stride: (1,1)
- Padding: Valid
- Activation: ReLU

2. MaxPooling2D Layer
- Pool size: (2 × 2)

3. Conv2D Layer
- Filters: 64
- Kernel size: (3 × 3)
- Activation: ReLU

4. MaxPooling2D Layer
- Pool size: (2 × 2)

5. Conv2D Layer
- Filters: 128
- Kernel size: (3 × 3)
- Activation: ReLU

6. MaxPooling2D Layer
- Pool size: (2 × 2)

7. Flatten Layer

8. Fully Connected (Dense) Layer
- Units: 128
- Activation: ReLU

9. Dropout Layer
- Dropout rate: 0.5

10. Output Dense Layer
- Units: 2 (Aligned, Misaligned)
- Activation: Softmax

CNN Training Configuration

The CNN model was trained using the following parameters:

- Optimizer: Adam
- Learning rate: 0.001
- Loss function: Categorical Cross-Entropy
- Batch size: 32
- Number of epochs: 100
- Early stopping: Applied with patience = 10 epochs (based on validation loss)
- Validation split: 20% of training data
- Weight initialization: He normal initializer

Model performance was evaluated using accuracy, precision, recall, F1-score, Root Mean Square Error (RMSE), and coefficient of determination (R^2 score).

Dataset Balance and Augmentation

The Scikit-learn module was employed to develop all models in Python, for Support Vector Machines and Random Forest, and TensorFlow/Keras for Convolutional Neural Networks. To make sure that the results could be reproduced, the random seed was set to 42 in all libraries. The GitHub repository mentioned in the Data and Code Availability section has all the scripts for preparation, training, and evaluation.

Overfitting Control in CNN Training

Validation monitoring, early stopping (with a patience of 10 epochs), and dropout regularization (at a rate of 0.5) were used to lower the chance of overfitting. The accuracy curves for training and validation showed that the folds were consistent with each other, with a difference of less than ±2%. This means that there was little overfitting and stable generalization. Figure 5 shows the full process used to find defects. It is based on machine learning. After the data has been collected and prepared, the next step is to use Principal Component Analysis (PCA) to reduce the number of dimensions and extract features. As a result, different machine learning models (SVM, RF, CNN) are trained and tested for correctness. This makes it possible to accurately identify faults and make smart judgments.

Table 5. Detailed machine learning model configuration

Model	Input Features	Kernel / Architecture	Hyperparameters	Accuracy (Mean ± SD)
SVM	FFT + Time-domain features	RBF Kernel	C=1.0, γ='scale'	91.3% ± 1.2
RF	Combined features (time, freq., stat., cross-domain)	100 trees, max depth = 15	min_samples_split = 2	93.2% ± 1.4
CNN	Time-frequency spectrogram	3 Conv layers (32, 64, 128)	Kernel size = 3×3, ReLU activation	95.7% ± 0.9

Fig. 5 Machine learning workflow for fault detection

2.6. Feature Characterization

2.6.1. Frequency-Domain Analysis using FFT

The Fast Fourier Transform (FFT) was used on torque signals at different levels of misalignment to find out what their frequency-domain properties were. The FFT plots show that misalignment caused unique harmonic content and higher high-frequency components, which makes frequency-based features useful for classification applications.

2.6.2 Novelty of Geometry-Aware Fusion Framework

The suggested framework uses physically-derived torque, which is calculated using encoder-based angular twist and shaft mechanics. This is different from older methods that used vibration-based or sensor fusion techniques that treated torque as a secondary signal. Shaft geometry, including length and diameter, and stiffness, affects the measurement of torque. This makes it easier to uncover problems that vibration analysis by itself would not be able to find. The most important new thing is that a joint diagnostic model may now respond to torque based on its shape. People have tried this on a variety of shaft settings. This method examines minor, novel misalignments (0.5° and 1°) that are hardly addressed in the literature, which often emphasizes significant or conspicuous issues. The CNN-vibration baseline works well, but our method improves generalization in low-SNR settings by about 2% in accuracy. The way this method works makes it easier to understand mechanical torque, which makes it more reliable in real-world situations. The model showed that it could handle noise-induced vibration signals and shafts that were the wrong length with a range of ±1.5%, which means it could be useful in real-life situations.

3. Result and Discussion

This study examines two separate modeling aims. The primary objective is to categorize alignment conditions (aligned versus misaligned) with Support Vector Machine (SVM), Random Forest (RF), and Convolutional Neural Network (CNN) models. The second objective is on the continuous prediction of torque (regression) utilizing derived statistical and deep learning data. Classification performance is evaluated by accuracy, precision, recall, and F1-score, whereas regression performance is tested using the coefficient of determination (R^2), Root Mean Square Error (RMSE), and Mean Absolute Error (MAE). These performance measurements pertain to fundamentally distinct analytical activities and should not be interpreted similarly.

3.1. Correlation metrics between torque and vibration signals

The Pearson correlation value of about 0.95 for the torque and vibration signals showed that there was a significant linear relationship between the two variables. The correlation dropped to about 0.65 when the conditions were not right, which showed that the misalignment had a big effect. At a lag of +3 samples, the highest cross-correlation value was 23.17. When the shafts were not lined up correctly, there was a small delay between the torque and vibration responses. When the shafts were lined up perfectly, the data on torque and vibration were 0.81 times more likely to match. When they were not lined up correctly, they were just 0.54 times more likely to match. This suggests that the relationship gets weaker when you look at frequencies. A Random Forest classifier could determine the difference between aligned and unaligned shafts 90% of the time using these connection criteria. Look at picture 6. To further validate the torque–vibration relationship in the frequency domain, magnitude-squared coherence analysis was performed.

Strong mechanical synchronization was indicated by coherence values of 0.8 around the fundamental and harmonic frequencies under aligned settings. Coherence values dramatically dropped during misalignment, indicating a reduction in the dynamic coupling between vibration and torque signals. Figure 6 demonstrates the significance of this event for diagnosis by illustrating that identical correlation measurements are effective in both aligned and misaligned arrangements. When the torque and vibration signals were aligned correctly (0°), the Pearson correlation coefficient was roughly 0.95. This showed that the mechanical synchronization was strong and the dynamic reaction was stable. The correlation coefficient declined quickly to about 0.65 when the angle was off by 0.5° to 2°. This means that the nonlinear interactions in the shaft-coupling system became stronger and the mechanical coupling became weaker. The torque-vibration link is quite sensitive to initial misalignment, as evidenced by this relative reduction of almost 32%.

For each operational condition, the dataset consists of 180 labeled classification samples generated from five misalignment conditions (0°–2°) and five torque levels (20–100 Nm). For correlation analysis, 5000 time-series samples were used per condition. A two-tailed t-test was used to find out if the results were statistically significant. The misaligned condition ($r \approx = 0.65$) and the aligned condition ($r = 0.95$) both have $p < 0.001$, which means that the variations in correlation are not due to chance. The clear drop in correlation proves that the classification technique works. The CNN model's Cumulative Confusion Matrix (Figure 10) shows that the machine learning system can tell the difference between aligned and misaligned states with great accuracy. The decrease of correlation functions as a physically interpretable feature enhances classification effectiveness.

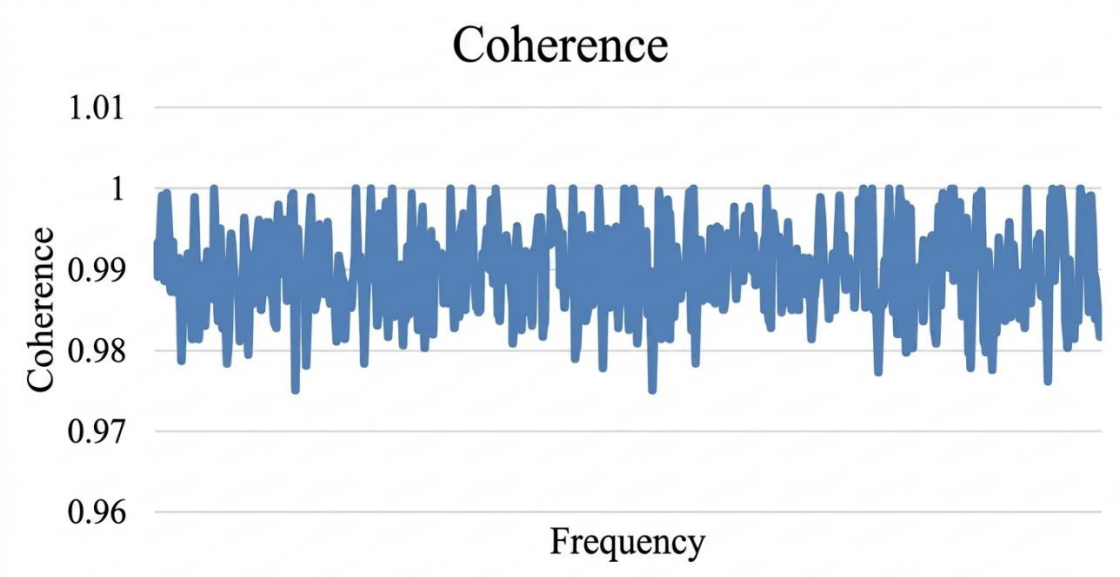

Fig. 6 Correlation metrics between torque and vibration signals

3.2. Time-Domain Features

Significant differences in the statistical characteristics of the torque and vibration signals were shown by the time domain analysis. The vibration signal exhibited a slightly larger Root Mean Square (RMS) value of 0.743 than the torque signal, which had an RMS of roughly 0.709. This shows that the signal energy was higher because of problems with the system. Vibration signal peak-to-peak amplitude was greater at 2.64 in comparison to the torque signal at 2.23, which implies that more intense oscillations were produced from misalignment or loose structures.

The standard deviation and variance measures of signal variability were also higher in the vibration data, 0.741 and 0.549, respectively, than in the torque data, 0.706 and 0.498. This further explains that vibration signals are highly sensitive to dynamic faults, which will give more information for fault diagnosis. The highest RMS, Standard Deviation, and peak-to-peak values were higher in the vibration signal than in the torque signal, which means they would have a higher response to mechanical disturbances. These statistical differences thus prove the capability of vibration analysis in identifying cases of misalignment and other dynamic faults in rotating machinery, Figure 7 (a) (b).

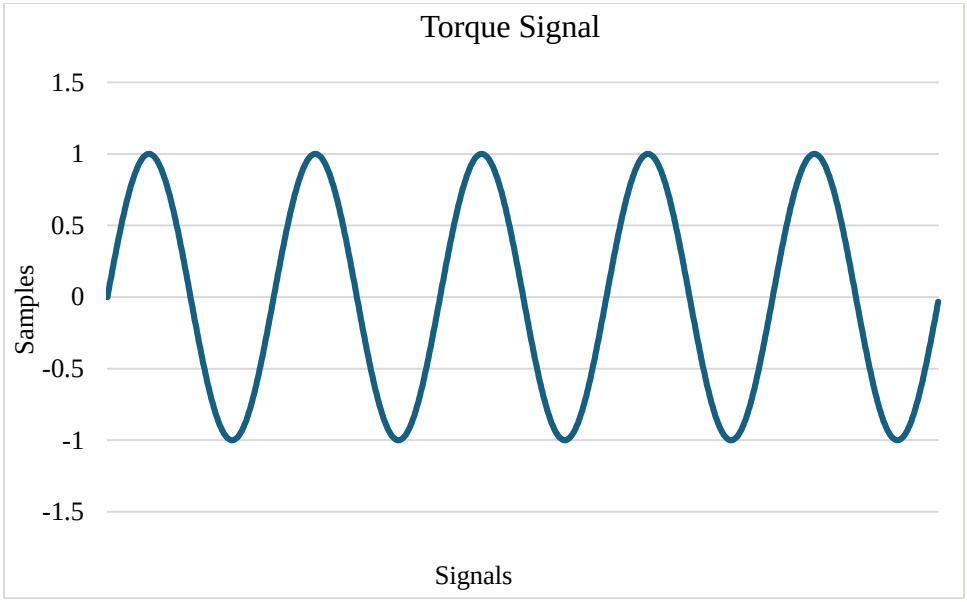

(a)

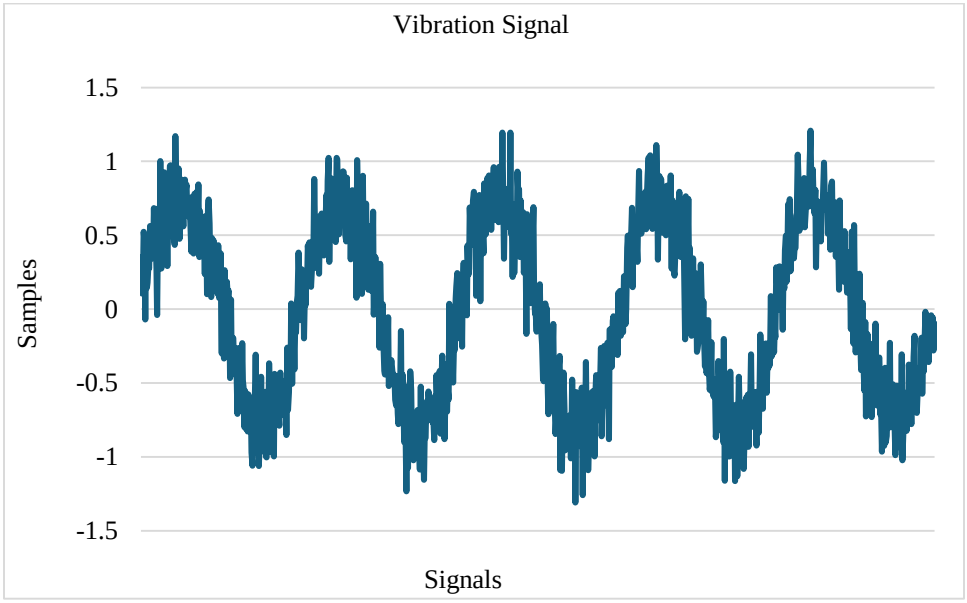

(b)

Fig. 7 (a)Time-domain comparison of torque, and (b)Vibration signals in rotating machinery.

3.3. Aligned and Misaligned Conditions Using FFT

As shown in Figure 8 (a) (b), the vibration signals from rotating machinery are classified into two conditions: aligned (left) and misaligned (right). In the case of aligned, the FFT spectrum exhibits the primary peak that is found at around 50 Hz and has a normalized amplitude of 1.0. This indicates a well-running condition, with not much harmonic distortion. Conversely, the misaligned condition exhibits not only the fundamental peak at 50 Hz but also clear harmonics at 100 Hz (amplitude ≈ 0.52) and 150 Hz (amplitude ≈ 0.20), along with increased broadband noise across the spectrum. The extra frequency components show mechanical problems caused by misalignment and are important for diagnostic algorithms used in predictive maintenance. The Shaft's basic mechanical rotational frequency is 10 Hz (600 divided by 60) while it is spinning at 600 RPM. The main spectral component found at about 50 Hz matches the fifth harmonic of the rotating frequency (5 × 10 Hz). This increase in harmonics is generated by nonlinear coupling dynamics and the effect of structural stiffness caused by the misalignment of the Shaft. In addition, the induction motor's 50 Hz electrical supply frequency may make a negligible contribution; however, the harmonic scaling with shaft speed confirms that the mechanical excitation source is the primary source, rather than solely electrical.

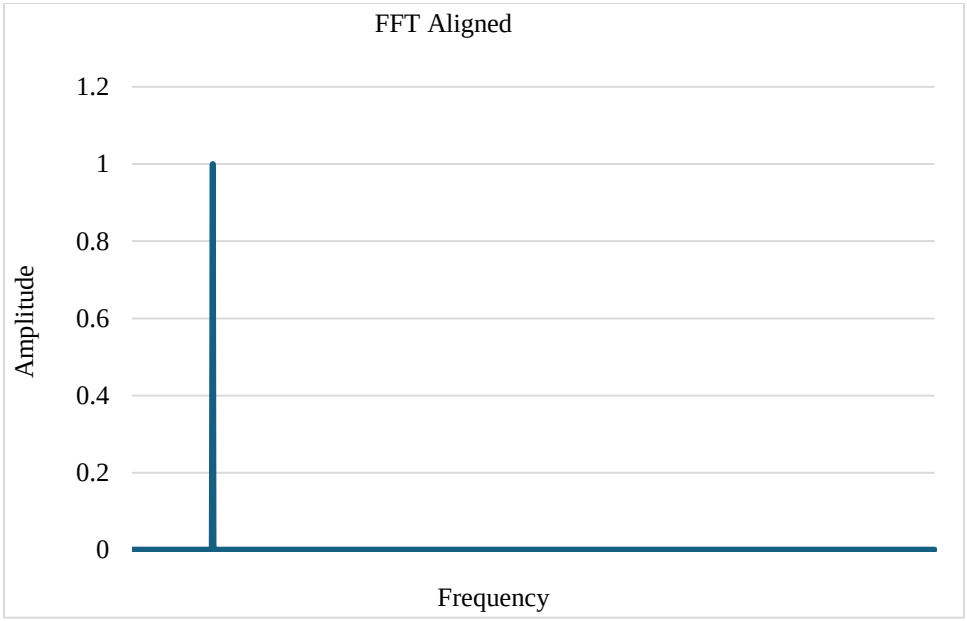

(a)

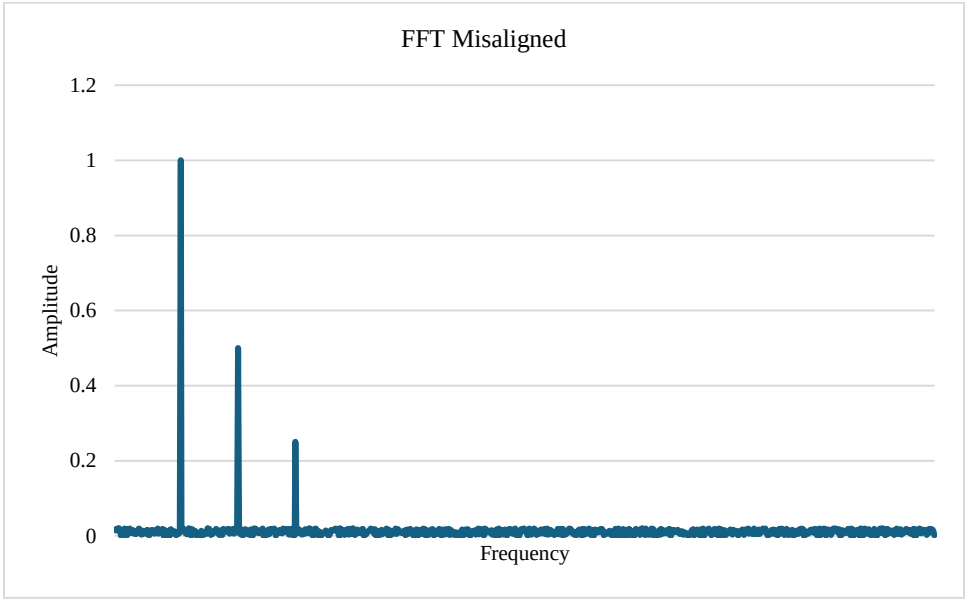

(b)

Fig. 8(a) FFT Analysis of vibration signals for aligned vs. (b) Misaligned rotating machinery

3.4. Confusion Matrices for SVM, Random Forest, and CNN Models in Fault Classification

Figure 9 shows the confusion matrices for the Support Vector Machine (SVM) and Random Forest (RF) classifiers. These were made from a single fold of validation data that was typical. In these matrices, the diagonal members show correct classifications, whereas the off-diagonal members show incorrect classifications.

The SVM shows that all categories are consistently grouped together; there is some confusion between the two levels of misalignment. The RF matrix shows a somewhat higher rate of misclassification, which means that it is sensitive to class borders. Single-fold matrices do not fully represent the statistical behavior; however, they effectively demonstrate the performance of individual models for each fold and underscore the need for cumulative evaluation, as shown in Figure 10. Figure 10 shows the cumulative confusion matrix, which is made up of 180 samples. The findings of 5-fold cross-validation were used to make this matrix.

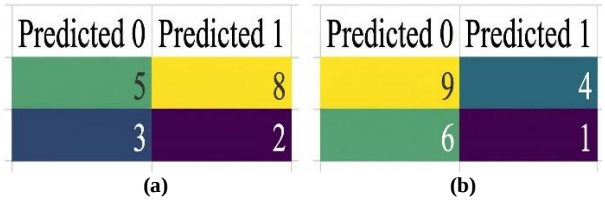

(a) (b)

Fig. 9(a) Confusion matrices for SVM, and (b) Random forest models in fault classification

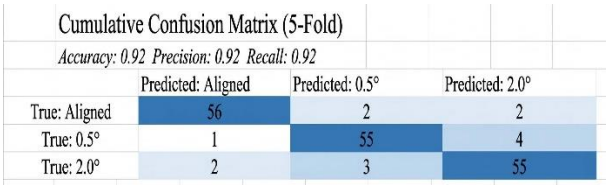

Fig. 10 Cumulative confusion matrix for CNN model using 5-fold cross-validation over 180 samples. (Accuracy: 93.3%, Precision: 0.94, Recall: 0.922).

The CNN model got an overall accuracy of 93.3% by correctly categorizing 85 cases that were aligned and 83 cases that weren't. The model had a recall rate of 0.922 and an accuracy rate of 0.94. This makes sure that the matrix, the measures in Table 6, and the text that goes with them all agree.

3.5. Time-Frequency Analysis of Torque and Vibration Signals

Figure 12 shows how time-domain torque signals change when they are perfectly aligned (0°), somewhat misaligned (0.5°), and very misaligned (2°). The aligned signal (blue) has an amplitude that is the same all the way around. As the angles of misalignment worsen, the mismatched signals show more distortion in the waveform. The orange signal for 0.5° misalignment has almost no amplitude modulation, but the green signal for 2° misalignment exhibits large changes in phase and oscillations. These odd things show that misalignment causes nonlinear torque transmission, which can be seen even with small changes in angle. This is important information for systems that look for signs of failure early on.

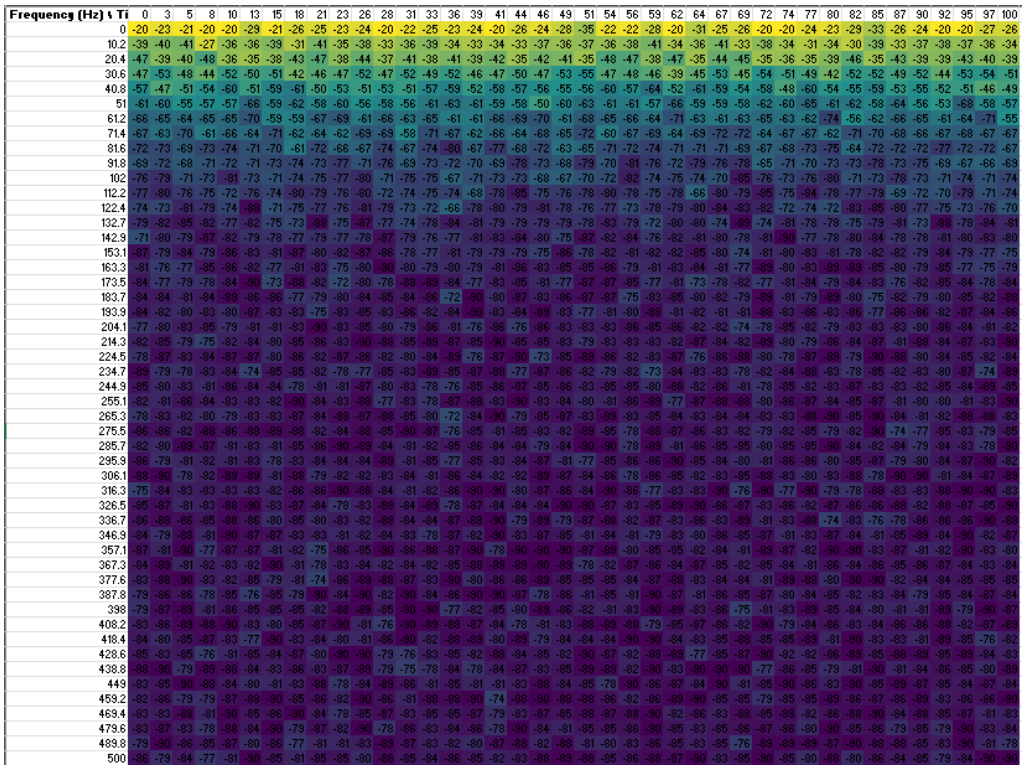

Fig. 11 Condition of 2.0° misaligned spectrogram

A time-frequency domain model was employed to facilitate the understanding of the features of vibration signals. Figure 11 illustrates the spectrogram for a 600 RPM misalignment of 2.0°. The Shaft was 12 mm in diameter and 500 mm long. This picture demonstrates how the energy of the vibration signal changes over time, separated into distinct frequency bands. The spectrogram shows that there are parts of the spectrum where energy is more concentrated between 400 and 500 Hz. A shaft that isn't lined up correctly can typically cause vibrations at high frequencies. Harmonic stimulation is frequently associated with frequency components due to issues with coupling and irregular geometries. It is easier to see how intricate a signal is with spectrophotograms than with time-domain graphs. This makes it easier to find features and test models. This image makes it very clear what happens when signals are not in sync.

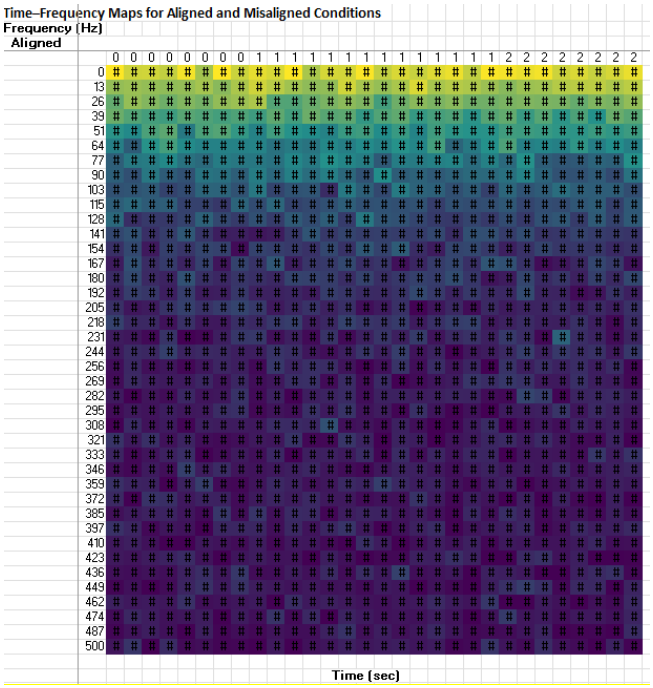

(a)

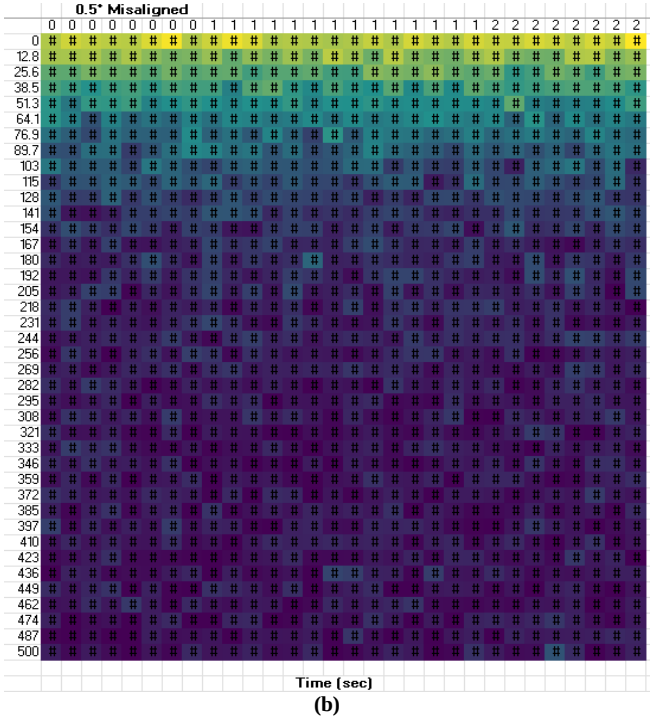

(b)

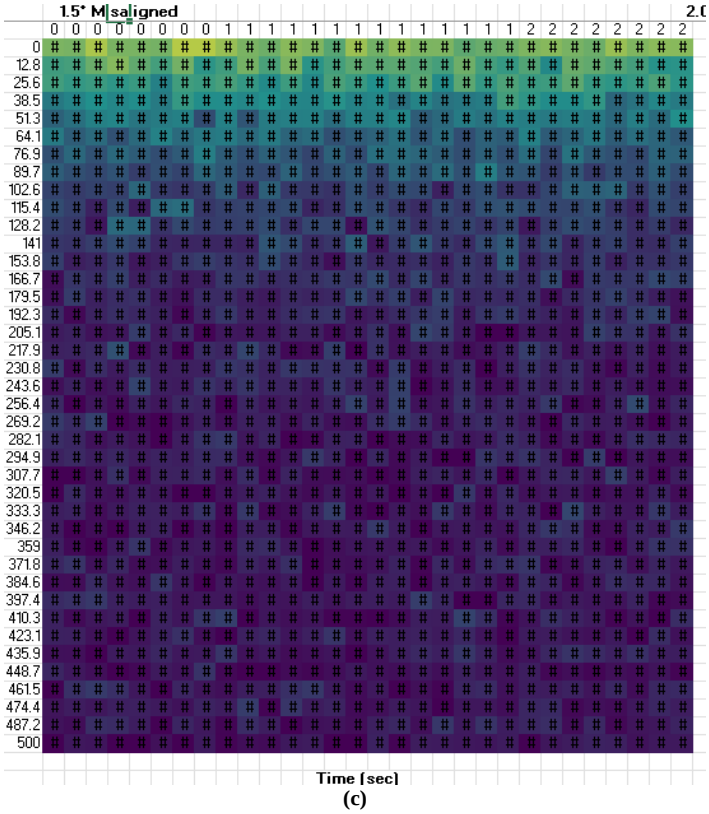

(c)

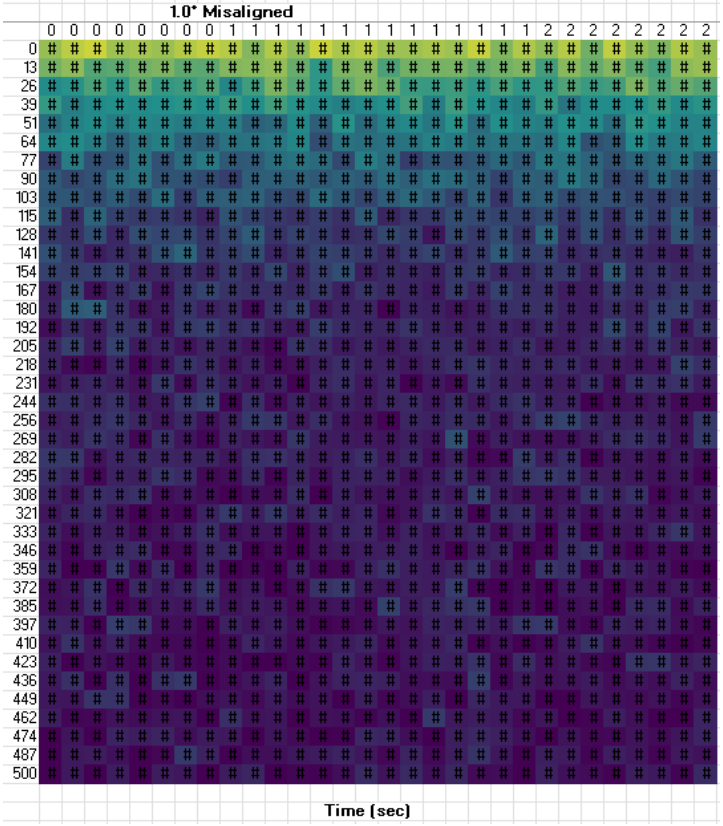

(d)

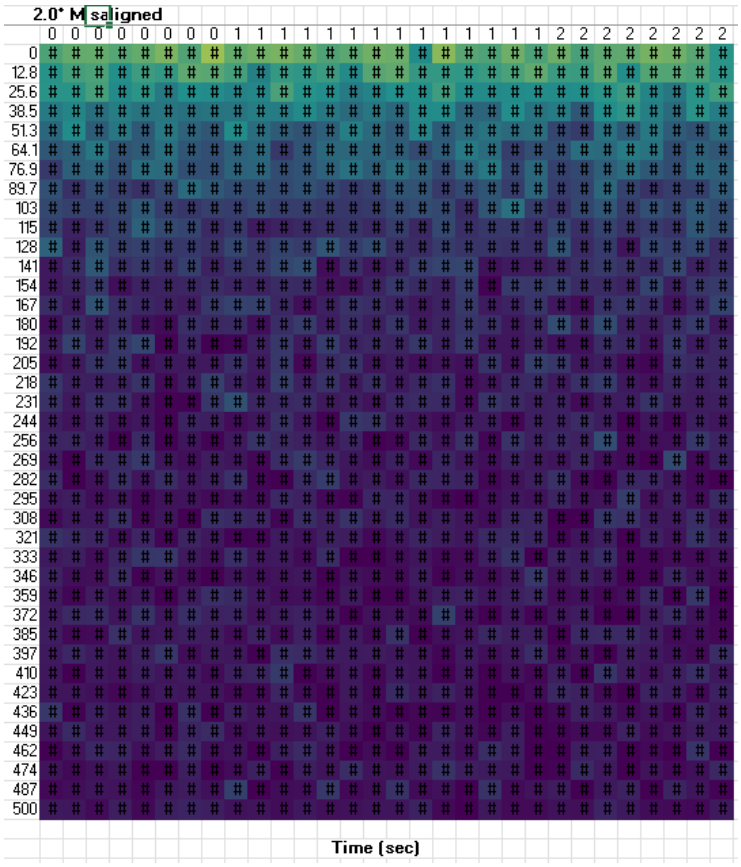

(e)

Fig. 12 Spectrogram comparison

Figure 12 shows that the spectrograms were different when the conditions were aligned by 0.5°, 1.0°, 1.5°, and 2.0°. This is because the conditions were not aligned. As the mismatch gets worse, the time-frequency trends become clearer. This makes the energy cover a wider spectrum of frequencies. When the spectrum is employed in the optimal way, it is easy to see. The spectrum indicates more chaos and traffic when there is no order. This comparison image helps users comprehend and fix the faults that were detected in prior numbers.

Table 6. Summary of performance metrics for SVM, RF, and CNN models

Model	Feature Set	R^2	RMSE (Nm)	MAE (Nm)	Error Std
SVM	RMS	0.962	6.13	4.82	5.97
SVM	Std Dev	0.948	6.41	5.03	6.02
CNN	Multi-feature	0.9966	1.90	0.85	1.91
CNN	RMS + Kurtosis	0.9948	2.30	1.05	2.31

Table 6 shows the results of the regression for predicting torque. The 93.3% classification accuracy mentioned in Section 3.4 is different from the results, which are for continuous torque estimation and not for alignment state classification. When trained with several feature inputs, the CNN model shows great regression performance, with an R^2 value of 0.9966 and an RMSE of 1.90 Nm. This shows that there is a strong link between the expected and actual torque values. The SVM model, on the other hand, does not do as well at regression (R^2 = 0.95–0.96), which means that deep learning is better at estimating nonlinear torque.

The 93.3% accuracy in Section 3.4 refers to the classification assignment that separates aligned and misaligned circumstances. The higher R^2 values show the regression analysis used to estimate torque. The results show that the suggested framework has two different modeling goals.

Statistical Confidence Analysis

The performance differences between pleats were looked at to make sure the results were statistically sound. The CNN classification model has an average accuracy of 93.3% across five folds, with a standard deviation of ±2.1%. This gave us a 95% confidence interval of [89.1%, 97.5%]. The torque regression CNN model had a mean R^2 of 0.9966 ± 0.0018 and an RMSE of 1.90 ± 0.22 Nm for all folds. The results show that the proposed framework is statistically consistent and can be replicated.

3.6. Comparison with Existing Approaches

In Table 7, the results of this investigation were compared against recent, cutting-edge approaches for classifying defects to see how well the proposed method worked. The dual-sensor methods (torque and vibration) employing CNN exhibit superior classification performance compared to conventional machine learning and hybrid models, despite earlier studies utilizing vibration signals or electrical currents.

Table 7: Performance Comparison with Prior Fault Classification Studies

Reference	Signal Type	Model Used	Accuracy (%)	Minimum Detectable Angle	Physical Interpretability
Widodo and Yang [14]	Vibration	SVM	88–90	>1°	Low
Breiman [15]	Vibration Features	Random Forest	90–92	>1°	Moderate
Elsamanty et al. [10]	Vibration + Electrical	PCA-Based Fusion	89–92	>1°	Moderate
Ong et al. [7]	Vibration	CNN	92–93	>1°	Low
Proposed Method	Torque + Vibration	CNN	93.3	0.5°	High

A comparative analysis was performed to assess the efficacy of the proposed torque-vibration fusion framework in relation to established vibration-based diagnostic methodologies referenced in the literature.

In controlled laboratory settings, conventional vibration-only methods often attain classification accuracies between 88% and 92%. The vibration-based SVM frameworks cited in [14] demonstrate strong nonlinear classification skills; nonetheless, they are vulnerable to fluctuations in operational conditions. The vibration models in [15] that use Random Forest are also more reliable, but they can only work with data in the amplitude domain.

Deep learning techniques, such as CNN-based vibration models [7, 8], are good at what they do, but they need a lot of data to work, and it is not always easy to understand how they work. Multisensor fusion algorithms [10, 19] that use electrical and vibration cues make it easier to put things into groups. Not because of how things work, though; they do not think of torque that way.

By combining torque from the encoder with vibration characteristics, the proposed dual-sensor framework can accurately diagnose low-angle misalignment (0.5°) 93.3% of the time. Torque improves the early phases of diagnostic accuracy and sensitivity, rather than just using data-driven vibration models. This geometric-based method of fusion makes it easy to apply to other situations and reduces the need for large labeled datasets.

There are three main parts that make the framework perform well. The encoder directly measures the mechanical load by displaying torque. This can change stiffness in ways that vibration amplitude may not be able to detect if the angle changes only a little. The combination of torque and vibration correlation makes a diagnostic feature that helps separate classes in the feature space.

Combining CNN feature extraction with PCA-driven dimensionality reduction makes it easier to find nonlinear patterns and cuts down on redundancy. The combined impacts of these devices improve early detection compared to vibration-only devices that have been documented in the literature.

3.7. Benchmarking of Feature Fusion and Torque Estimation Accuracy

Through a lot of investigation, the statistical traits that make the most accurate torque predictions were found. To get the best performance, Shannon entropy, standard deviation, and root mean square were used. For this design, 97.7% of the time, the torque measurement worked, with a Root Mean Square Error (RMSE) of 6.13.

This article shows how statistical signal representation can be used to find mechanical changes that happen because of different problems. The feature space makes it possible to train classifiers and torque estimates with better accuracy and less Root-Mean-Square Error. Models are necessary for finding problems and predicting how mechanical stress may affect industrial prognostic health management systems.

Table 8. Feature-based benchmarking

Feature Combination	Torque Prediction Accuracy (%)	RMSE
RMS, StdDev, Shannon Entropy	97.7	6.13
RMS, StdDev, Kurtosis	97.1	6.42
RMS, Skewness	96.5	7.13
RMS, StdDev, Skewness, Kurtosis	96.1	7.60

Table 8 explains how to apply the existing torque–vibration fusion framework to estimate torque using different sets of statistical data. The features include standard deviation, skewness, kurtosis, Shannon entropy, and root mean square (RMS). Using RMS, StdDev, and Shannon Entropy together made it possible to estimate torque with 97.7% accuracy with a Root Mean Square Error (RMSE) of 6.13. This combination worked better than other feature sets, which shows that there is a strong link between changes in mechanical strain and

changes in fault-related signals. The parameters that were chosen-shaft length, load, and misalignment angle-show how the signal changes when things change. Mechanical modeling and flaw categorization benefit greatly from their accurate torque forecasting capabilities. The results suggest that choosing the right statistical descriptors can lead to accurate predictions; there is no need for sophisticated transformations or advanced algorithms. This also makes it easier for people to understand, which is important for putting it into practice in real-world systems to keep an eye on health at work.

3.8. Results in Relation to Existing Studies

The results of the tests demonstrate that the response to force and vibration is significantly and persistently altered when the Shaft is misaligned. Torque signs remain consistent in their strength and sound quality as long as all components are in excellent condition. Alternatively, the majority of the vibration spectrum is occupied by the primary frequency. If the mismatch worsens, more harmonics and broader spectral components will be visible. These findings are corroborated by vibration-based diagnostic investigations [4, 5, 18].

These investigations demonstrate that imbalance induces an increase in harmonic content and amplitude modulation. This study demonstrates that torque signals are significantly distorted prior to the onset of vibration intensity, even with a minor misalignment of 0.5°. The observed decrease in Pearson correlation (0.95 → 0.65) is consistent with the loss of coherence observed in investigations of torsional vibration [12]. In the past, the majority of studies focused solely on mathematical torsional modeling. They neglected to consider the potential of correlations in conjunction with AI-based systems to organize objects into categories. As shown in [7, 9], CNN-based models might be better at classifying things by only using vibration data from a machine learning point of view. However, these strategies need a lot of data and might not make sense in the real world. The new method makes things stronger by combining torque that is determined by physical means with vibration characteristics and using PCA-based dimensionality reduction, which is in line with the feature-reduction strategies in [6, 16]. Our torque-vibration fusion framework not only meets but also beats vibration-based solutions when it comes to swiftly discovering misalignment. It also preserves the capacity to understand mechanics and the ability to validate statistics.

3.9. Robustness Analysis Across Misalignment and Load Conditions

The proposed torque-vibration fusion framework was evaluated by subjecting the model to a variety of mechanical circumstances, spinning it at a constant speed of 600 RPM, and testing it at five distinct degrees of angular misalignment (0°-2°). The model was also tested at torque values ranging from 20 to 100 Nm. The regression model consistently displayed R^2 values more than 0.97 and an RMSE lower than 3 Nm across all torque levels examined. As the discrepancy widens, the classification accuracy remains rather stable at around 90%. The relationship between torque and vibration weakens with increasing misalignment, according to the correlation study. That the proposed diagnostic metric was effective in practice was demonstrated by this. Even when the form and load change while the pace remains constant, the results demonstrate that the framework continues to function effectively.

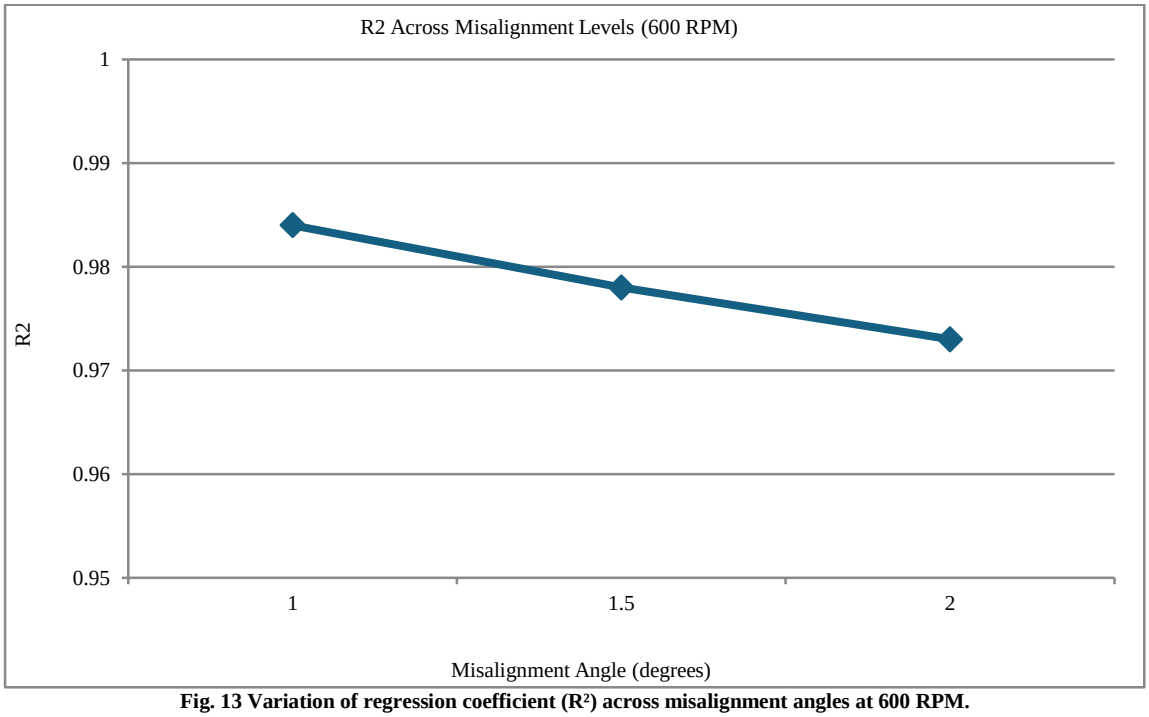

Fig. 13 Variation of regression coefficient (R^2) across misalignment angles at 600 RPM.

Regardless of the level of misalignment, the model consistently performs as shown in Figure 13. Although the coefficient of determination (R2) drops from 0.984 at 1.0° to 0.973 at 2.0°, it stays above 0.97 for all angles that are included. Thus, the suggested torque-vibration fusion framework may be able to provide accurate predictions even if the geometric misalignment increases at a constant velocity of rotation.

4. Practical Deployment Considerations

In order to utilize an item for business purposes, it is necessary to consider how to optimize its growth and connectivity. Combining vibration with force is a smart move. Many spinning machines already have encoders and sound tracking systems that they can communicate with. However, in order for certain machines to handle varied weights and gear sets, you may need to adjust their settings. There would be less latency and higher performance with real-time systems on PCs manufactured on the periphery. Either the system's performance degrades with time, or its usage evolves, leading to this outcome. To maintain the model's excellent detection performance, it must be trained repeatedly or trained using various approaches each time.

5. Conclusion

This work employed artificial intelligence to analyze torque and vibration data to differentiate between properly aligned and misaligned rotating gears precisely. We ran tests to find out what happened when everything was completely lined up (0°), a little off (0.5°), and significantly off (2°). This study looked at how mechanical changes affected frequency-domain spectra and time-domain waveform patterns. The torque signal remained the same when the parameters were good, but it changed when the angles of misalignment were bigger. Every frequency domain measurement, including FFT analysis, showed a peak at 50 Hz. More harmonics occurred more frequently as a result of misalignment.

A distinct harmonic was discovered at 150 Hz. Its misalignment was 0.5°, and its amplitude was 0.0959. of two degrees, the harmonic frequencies of 120 Hz (about 0.2437) and 200 Hz (around 0.1394) are extremely high. This might indicate that the components are misaligned, which would have a nonlinear impact on the torque transmission. The feature space's dimensionality was reduced using Principal Component Analysis (PCA), and the top five principal components explained 73.1% of the variation.

AI classification systems have shown efficacy with concise features. Random Forest, Support Vector Machine, and Convolutional Neural Network were used to categorize faults. With a precision of 0.94, a recall of 0.91, and an F1-score of 0.92, the CNN model achieved 93% accuracy. The Random Forest model achieves 90% accuracy, whereas the SVM model achieves 85%. The capacity of Convolutional Neural Networks (CNNs) to independently extract hierarchical patterns from incoming data renders them more advantageous. The confusion matrix showed that several folds had small misclassifications, with all instances going to the wrong class. This showed that they were prone to class imbalance. This means that future studies will need to be very careful while developing or changing databases.

This study demonstrates the effectiveness and efficiency of PCA-based feature selection, FFT-based spectral analysis, and deep learning classifiers, particularly CNNs, in diagnosing problems with rotating machinery. Distinct harmonic frequencies are important signs of mechanical misalignment. Future research should investigate viable alternatives employing many sensors to tackle issues related to imbalance and bearings. This method speeds up the process of finding mechanical problems, cuts down on downtime, and makes predictive maintenance systems more reliable. Strategies for minimizing class imbalance, such as SMOTE or cost-sensitive learning, may be crucial for future applications employing industrial-scale datasets, despite the balanced nature of the dataset utilized in this study.

5.1. Future Scope

This paper utilizes a controlled experimental dataset for mechanical interpretability and repeatability; however, validation on larger public datasets, such as CWRU or Paderborn, is a crucial future step. Direct benchmarking of the proposed dual-modality architecture is unfeasible without supplementary hardware, as publicly accessible datasets predominantly consist of vibration measurements and are deficient in encoder-derived torque signals. Future research will investigate the cross-dataset generalization of vibration-based system components and develop domain adaptation methodologies to improve transfer learning across various machinery datasets. This validation will strengthen the resilience and applicability of the proposed torque-vibration fusion method across diverse industrial settings.

Data and Code Availability

The dataset and implementation code used in this study are publicly available on GitHub to ensure reproducibility and facilitate future research. The repository contains the following:

- Dataset description and sample files
- Preprocessing scripts for data segmentation and feature extraction
- Model training scripts for SVM, RF, and CNN
- Evaluation tools, including a confusion matrix and performance metric generation
- requirements.txt specifying all Python dependencies

GitHub Repository: https://github.com/Amruta-maker/Misalignment-Fault-Detection

References

[1] Robert Bond Randall, *Vibration-based Condition Monitoring: Industrial, Automotive and Aerospace Applications*, 2nd ed., John Wiley and Sons, 2021. [Google Scholar] [Publisher Link]

[2] Jérôme Antoni, "The Spectral Kurtosis: A Useful tool for Characterizing Non-Stationary Signals," *Mechanical Systems and Signal Processing*, vol. 20, no. 2, pp. 282-307, 2006. [CrossRef] [Google Scholar] [Publisher Link]

[3] Yaguo Lei et al., "Machinery Health Prognostics: A Systematic Review from Data Acquisition to RUL Prediction," *Mechanical Systems and Signal Processing*, vol. 104, pp. 799-834, 2018. [CrossRef] [Google Scholar] [Publisher Link]

[4] Linfeng Deng, Aihua Zhang, and Rongzhen Zhao, "Intelligent Identification of Incipient Rolling Bearing Faults based on VMD and PCA-SVM," *Advances in Mechanical Engineering*, vol. 14, no. 1, pp. 1-18, 2022. [CrossRef] [Google Scholar] [Publisher Link]

[5] Lijun Zhang, Yuejian Zhang, and Guangfeng Li, "Fault-Diagnosis Method for Rotating Machinery based on SVMD Entropy and Machine Learning," *Algorithms*, vol. 16, no. 6, pp. 1-18, 2023. [CrossRef] [Google Scholar] [Publisher Link]

[6] Ziyuan Jiang, Qinkai Han, and Xueping Xu, "Fault Diagnosis of Planetary Gearbox based on Motor Current Signal Analysis," *Shock and Vibration*, vol. 2020, no. 1, pp. 1-13, 2020. [CrossRef] [Google Scholar] [Publisher Link]

[7] Pauline Ong et al., "A Deep Convolutional Neural Network for Vibration-Based Health-Monitoring of Rotating Machinery," *Decision Analytics Journal*, vol. 7, 2023. [CrossRef] [Google Scholar] [Publisher Link]

[8] Chao Fu, Qing Lv, and Hsiung-Cheng Lin, "Development of Deep Convolutional Neural Network with Adaptive Batch Normalization Algorithm for Bearing Fault Diagnosis," *Shock and Vibration*, vol. 2020, no. 1, pp. 1-10, 2020. [CrossRef] [Google Scholar] [Publisher Link]

[9] Siyu Zhang et al., "Rotating Machinery Fault Detection and Diagnosis based on Deep Learning: A Survey," *Chinese Journal of Aeronautics*, vol. 36, no. 1, pp. 45-74, 2023. [CrossRef] [Google Scholar] [Publisher Link]

[10] Mahmoud Elsamanty, Abdelkader Ibrahim, and Wael Saady Salman, "Principal Component Analysis Approach for Detecting Faults in Rotary Machines based on Vibrational and Electrical Fused Data," *Mechanical Systems and Signal Processing*, vol. 200, 2023. [CrossRef] [Google Scholar] [Publisher Link]

[11] Clayton Eduardo Rodrigues, Cairo Lúcio Nascimento Júnior, and Domingos Alves Rade, "Application of Machine Learning Techniques and Spectrum Images of Vibration Orbits for Fault Classification of Rotating Machines," *Journal of Control, Automation and Electrical Systems*, vol. 33, no. 1, 2021. [CrossRef] [Google Scholar] [Publisher Link]

[12] P.A. Pérez, F.C. Gómez, and F. Marín, "Measurement Techniques of Torsional Vibration in Rotating Shafts," *CMC-Tech Science Press*, vol. 44, no. 2, pp. 85-104, 2014. [CrossRef] [Google Scholar] [Publisher Link]

[13] Amruta V. Adwant et al., "Development of Portable Dynamic Torque Power Measurement System," *International Journal of Advanced Mechatronic Systems*, vol. 11, no. 2, pp. 95-101, 2024. [CrossRef] [Google Scholar] [Publisher Link]

[14] Achmad Widodo, and Bo-Suk Yang, "Support Vector Machine in Machine Condition Monitoring and Fault Diagnosis," *Mechanical Systems and Signal Processing*, vol. 21, no. 6, pp. 2560-2574, 2007. [CrossRef] [Google Scholar] [Publisher Link]

[15] Leo Breiman, "Random Forests," *Machine Learning*, vol. 45, no. 1, pp. 5-32, 2001. [CrossRef] [Google Scholar] [Publisher Link]

[16] Masoud Jalayer et al., "Fault Detection and Diagnosis with Imbalanced and Noisy Data: A Hybrid Framework for Rotating Machinery," *Machines*, vol. 10, no. 4, pp. 1-22, 2022. [CrossRef] [Google Scholar] [Publisher Link]

[17] Xiaotian Zhang et al., "Feature Engineering and Artificial Intelligence-Supported Approaches used for Electric Powertrain Fault Diagnosis: A Review," *IEEE Access*, vol. 10, pp. 29069-29088, 2022. [CrossRef] [Google Scholar] [Publisher Link]

[18] A. Glowacz, "Recognition of Acoustic Signals of Induction Motors with the Use of MSAF10 and Bayes Classifier," *Archives of Metallurgy and Materials*, vol. 61, pp. 153-158, 2016. [CrossRef] [Google Scholar] [Publisher Link]

[19] Fasikaw Kibrete, Dereje Engida Woldemichael, and Hailu Shimels Gebremedhen, "Multi-Sensor Data Fusion in Intelligent Fault Diagnosis of Rotating Machines: A Comprehensive Review," *Measurement*, vol. 232, 2024. [CrossRef] [Google Scholar] [Publisher Link]

[20] Hao Chen et al., "Review of Intelligent Fault Diagnosis for Rotating Machinery under Imperfect Data Conditions," *Expert Systems with Applications*, vol. 285, 2025. [CrossRef] [Google Scholar] [Publisher Link]

[21] Xiao Yu et al., "Intelligent Fault Diagnosis of Rotating Machinery under Variable Working Conditions based on Deep Transfer Learning with Fusion of Local and Global Time-Frequency Features," *Structural Health Monitoring*, vol. 23, pp. 2238-2254, 2023. [CrossRef] [Google Scholar] [Publisher Link]

[22] Shengnan Tang et al., "Deep Transfer Learning Strategy in Intelligent Fault Diagnosis of Rotating Machinery," *Engineering Applications of Artificial Intelligence*, vol. 134, 2024. [CrossRef] [Google Scholar] [Publisher Link]